ELECTRONIC SUPPLEMENTARY INFORMATION

Phototransformation of anthraquinone-2-sulphonate in aqueous solution

Andrea Bedini,[a] Babita Sur,[a,b] Elisa De Laurentiis,[a] Valter Maurino,[a] Claudio Minero,[a] Marcello Brigante,*[c,d] Gilles Mailhot[c,d] and Davide Vione*[a,e]

[a] *Dipartimento di Chimica, Università di Torino, Via P. Giuria 5, 10125 Torino, Italy.* http://www.chimicadellambiente.unito.it

[b] *Department of Chemical Engineering, Calcutta University, 92 Acharya P. C. Road, Kolkata 700009, India.*

[c] *Clermont Université, Université Blaise Pascal, Institut de Chimie de Clermont-Ferrand, BP 10448, F-63000, Clermont-Ferrand, France.*
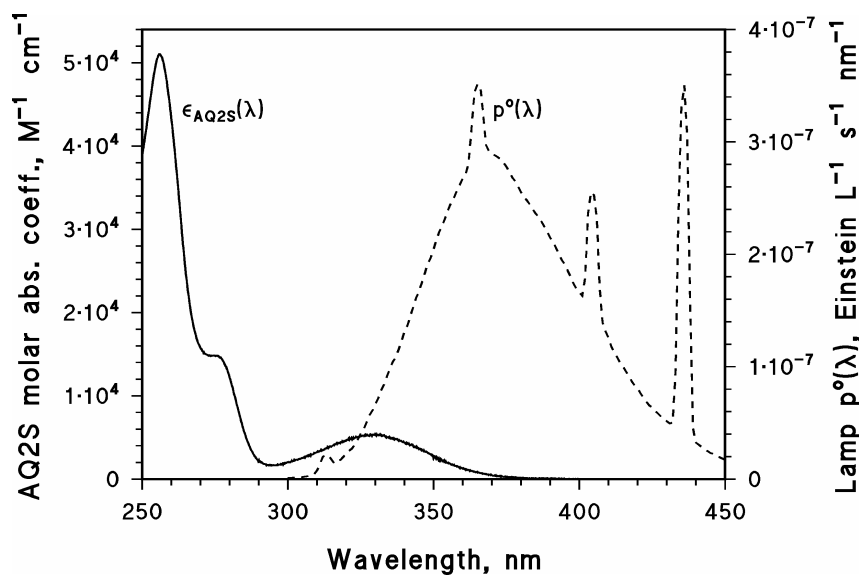
[d] *CNRS, UMR 6296, ICCF, BP 80026, Aubière, France.*

[e] *Centro Interdipartimentale NatRisk, Università di Torino, Via Leonardo da Vinci 44, 10095 Grugliasco (TO), Italy.* http://www.natrisk.org

* Address correspondence to either author.
marcello.brigante@univ-bpclermont.fr
davide.vione@unito.it

Figure ESI-1. Absorption spectrum of AQ2S (molar absorption coefficient $\varepsilon_{AQ2S}(\lambda)$). Emission spectrum of the UVA lamp (spectral photon flux density $p°(\lambda)$).[1]

[1] P. R. Maddigapu. A. Bedini, C. Minero, V. Maurino, D. Vione, M. Brigante, G. Mailhot and M. Sarakha, The pH-dependent photochemistry of anthraquinone-2-sulfonate, *Photochem. Photobiol. Sci.* 2010, **9**, 323-330.

Optimised structure features

The figure below shows the gas-phase optimised structure of anthraquinone-2-sulphonate (AQ2S) in its ground state (S_0). The bond lengths of both S_0 and T_1 states are also reported.
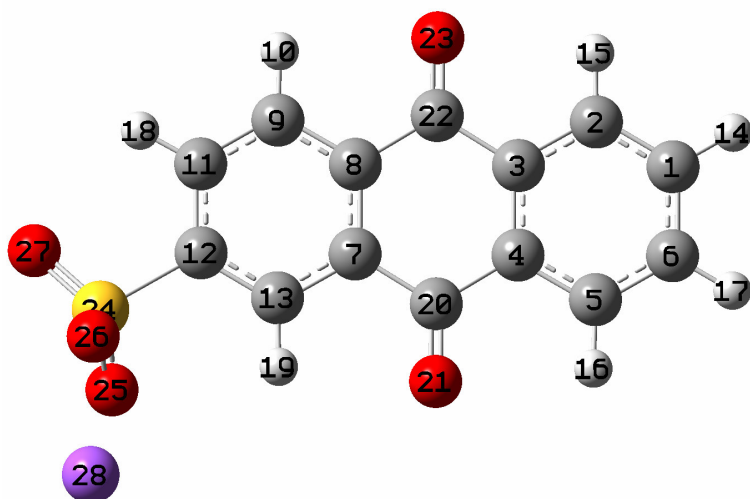

Figure ESI-2

Bond lengths for the optimised geometry of AQ2S in S_0 and T_1 states

Bond length (Å)	AQ2S (S_0)	AQ2S (T_1)
C22 – O23	1.2187	1.3023
C20 – O21	1.2200	1.2311
C1 – C2	1.3892	1.3795
C2 – C3	1.3976	1.4152
C3 – C4	1.4060	1.4161
C4 – C5	1.3978	1.4023
C5 – C6	1.3891	1.3836
C6 – C1	1.3974	1.4057
C7 – C8	1.4064	1.4162
C8 – C9	1.3968	1.4166
C9 – C11	1.3899	1.3766
C11 – C12	1.3953	1.4061
C12 – C13	1.3881	1.3819
C13 – C7	1.3945	1.4002
C7 – C20	1.4919	1.4767
C20 – C4	1.4914	1.4769
C3 – C22	1.4931	1.4416
C22 – C8	1.4924	1.4384
C1 –H14	1.0840	1.0841
C2 – H15	1.0829	1.0836
C5 – H16	1.0828	1.0834
C6 – H17	1.0840	1.0836
C9 – H10	1.0828	1.0836
C11 – H 18	1.0826	1.0826
C13 – H 19	1.0817	1.0822

S24 – C12	1.8090	1.8040
S24 – O25	1.5073	1.5076
S24 – O26	1.5085	1.5103
S24 – O27	1.4062	1.4609
O26 – Na28	2.2223	2.2167
O27 – Na28	2.2259	2.2235

The obtained structure has been compared to the XRD data collected by Gamage.[2] Bond lengths of the AQ2S skeleton calculated by us are comparable with the XRD ones: calculated and experimental data have an average absolute deviation of $1.9 \cdot 10^{-3}$ Å. Sulphur-oxygen distances are slightly overestimated by our calculation ($1.6 \cdot 10^{-2}$ Å as average absolute deviation), but the molecular structure optimised through the computation can be considered as a sufficiently good model for the real one.

Analysis of triplet state: geometry and spin densities

Also for AQ2S in its lower-lying triplet state (T_1) a geometry optimisation has been performed (see data reported above). A comparison with the bond lengths of the S_0 ground state shows that the length of C=O bond increases, confirming the incipient nature of the $>C–O^\bullet$ bond in the excited state. In particular the carbonyl group made of C22 – O23 atoms shows a more marked increase (0.08 Å) of bond length compared to the other carbonyl group (C20 – O21 atoms), which displays only a weak lengthening (0.01 Å). The S24 – O27 bond length (sulphonate group) shows an increase of 0.05 Å. To counterbalance these effects, a shrinking of the central six member carbon ring of the molecule is observed, where the C-C bonds in *alpha* to the carbonyl group tend to gain a more marked sp^2 character.

The total spin density surface of AQ2S T_1 is reported in Figure 2 of the manuscript and below.
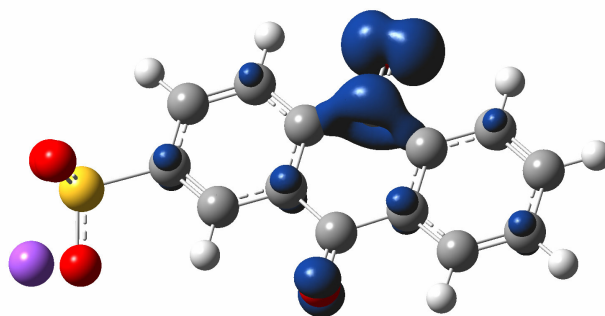
As can be seen, there are two main areas where the spin density is higher. The strongest one is centred on the carbonyl group (C22 – O23 atoms), the other one is on the atoms that allow the resonance of unpaired electrons on the aromatic skeleton of the molecule. In particular it can be

---

[2] R.S.K.A. Gamage, B.M. Peake, J. Simpson, *Aust. J. Chem.* **1993**, *46*, 1595-1604

observed that the spin density localised on O21 is itself the result of the resonance on the skeleton of AQ2S, due to the favourable position of the oxygen p orbital that is parallel to the aromatic π system.

The spin density of the carbonyl C22-O23 is curiously similar to that found on carbon monoxide in its lower-lying triplet state. Spin density is localised on the unoccupied π^* system of the carbonyl group, and its more roundish distribution around the C23 atom can be explained in terms of contribution of a carbon p orbital, due to the spin resonance over the aromatic skeleton of the molecule. Sulphur atoms and the associated oxygen atoms of the sulphonate groups, as well as hydrogen atoms, exhibit negligible spin density. Taking into account these considerations and previous results concerning the photoreactivity of anthraquinones,[3] we suppose that the two carbonyl groups of AQ2S are not equivalent from a reactivity point of view. We expect that the spin density on the carbonylic oxygen O23 accounts for AQ2S photochemistry, while the spin density delocalised over the aromatic skeleton is quite unreactive.

Mulliken atomic spin densities of AQ2S in its T_1 state

```
 1  C  -0.060528
 2  C   0.127620
 3  C  -0.011450
 4  C   0.135184
 5  C  -0.049643
 6  C   0.123136
 7  C   0.137618
 8  C  -0.009051
 9  C   0.128062
10  H  -0.006550
11  C  -0.056117
12  C   0.119624
13  C  -0.054817
14  H   0.003167
15  H  -0.006581
16  H   0.002694
17  H  -0.007093
18  H   0.002924
19  H   0.002779
20  C  -0.013281
21  O   0.193363
22  C   0.319862
23  O   0.972766
24  S  -0.005435
25  O   0.002204
26  O   0.006684
27  O   0.002812
28  Na  0.000047
```
Sum of Mulliken spin densities= 2.00000

---

[3] V. Maurino, A. Bedini, D. Borghesi, D. Vione, C. Minero, *Phys. Chem. Chem. Phys.* **2011**, *13*, 11213-11221

Excited states and electronic absorption spectrum

The TDDFT calculation was performed on AQ2S gas-phase optimised geometry to calculate the first 30 singlet and 30 triplet excited states. The purpose is to understand the behaviour of excited AQ2S by exploring the nature and position of its energy levels. TDDFT calculation was executed on the liquid phase, and the solvent effect was taken into account with the PCM method.

All the transitions from S_0 to a triplet state are forbidden by multiplicity rules and the related oscillator strength is zero. The lowest-lying triplet is positioned 2.6611 eV above the ground state of the molecule. The calculated absorption properties for AQ2S in the liquid phase are reported in Table ESI-1, where only transitions with an oscillator strength higher than 0.1 are described and compared with the experimental results. The obtained values are in very good agreement with experimental data as can be seen from the Table itself and from Figure 3 in the manuscript, which shows a fine match among experimental and simulated UV-VIS spectra of AQ2S in aqueous solution (both wavelengths and extinction coefficients).

Table ESI-1. Calculated absorption properties of AQ2S in water, where Transition[a] = as named from the calculation, E^b = excitation energy, λ^c = corresponding wavelength, f^d = oscillator strength (dimensionless quantity), ε^e = calculated molar absorption coefficient (10^4 M^{-1} cm^{-1}); λ_{exp}^f = band maximum wavelength from experimental UV-VIS spectra and ε^g = experimental molar absorption coefficient (10^4 M^{-1} cm^{-1}). Experimental results are from this work (UV-VIS spectra).

Transition[a]	E^b (eV)	λ^c (nm)	f^d	ε^e	Contributions	λ_{exp}^f (nm)	ε^g
S4	3.7192	333	0.1119	1.2417	H-2→LUMO (67%) HOMO→LUMO (5%) HOMO→L+1 (2%)	330	0.5782
S7	4.3378	286	0.1779	1.3118	H-6→LUMO (78%) H-4→LUMO (6%)	274	1.5803
S10	4.8585	255	0.5697	5.0491	HOMO→L+1 (65%)	256	5.0840
S19	5.7358	216	0.1376	1.0111	H-2→L+2 (40%), HOMO→L+2 (12%), H-6→L+3 (3%), H-4→L+3 (3%), H-2→L+3 (8%)	206	3.4207
S22	5.8491	212	0.1851	3.6674	H-5→L+2 (10%), H-4→L+2 (23%), H-3→L+2 (13%), HOMO→L+2 (16%), H-6→L+1 (4%), H-6→L+3 (3%), HOMO→L+3 (3%)	206	3.4207
S28	6.0182	206	0.1020	3.1345	HOMO->L+2 (35%), H-2->L+3 (9%)	206	3.4207

Calculated absorption properties of AQ2S (S$_0$), at the liquid-phase PCM level

First 30 excited singlet states

No.   Energy (eV)   Wavelength (nm)   Osc. Strength   Symmetry
Major and minor contributions (%)

1   3.0739   403.35   0.0   Singlet-A
H-1->LUMO (89%) H-5->L+1 (2%), H-2->LUMO (-2%)

2   3.3736   367.51   0.0   Singlet-A
H-5->LUMO (88%) H-1->L+1 (5%)

3   3.5648   347.8   0.012   Singlet-A
H-2->LUMO (-10%), HOMO->LUMO (78%)   H-4->LUMO (-2%)

4   3.7192   333.36   0.1119   Singlet-A
H-4->LUMO (-15%), H-2->LUMO (67%) HOMO->LUMO (5%), HOMO->L+1 (2%)

5   3.8366   323.16   0.0537   Singlet-A
H-4->LUMO (40%), H-3->LUMO (30%)   H-6->LUMO (-4%), H-6->L+1 (-2%),
H-2->LUMO (8%), HOMO->LUMO (9%)

6   3.8651   320.78   0.0159   Singlet-A
H-4->LUMO (-26%), H-3->LUMO (67%) H-2->LUMO (-2%)

7   4.3378   285.82   0.1779   Singlet-A
H-6->LUMO (78%) H-4->LUMO (6%)

8   4.5366   273.3   0.0   Singlet-A
H-1->L+1 (89%)   H-5->LUMO (-7%), H-2->L+1 (-2%)

9   4.7488   261.08   0.001   Singlet-A
H-7->LUMO (81%) H-8->LUMO (5%), H-5->L+1 (9%)

10   4.8584   255.19   0.5697   Singlet-A
HOMO->L+1 (65%) H-8->LUMO (-9%), H-2->L+1 (-3%), H-2->L+2 (-3%)

11   4.8748   254.34   0.0276   Singlet-A
H-7->LUMO (-12%), H-5->L+1 (79%)   H-1->LUMO (-2%), HOMO->L+1 (3%)

12   4.9279   251.6   0.0574   Singlet-A
H-8->LUMO (-10%), H-3->L+1 (23%), H-2->L+1 (56%) HOMO->L+2 (2%)

13   4.935   251.23   0.0006   Singlet-A
H-8->LUMO (15%), H-3->L+1 (69%), H-2->L+1 (-11%)

14   4.9418   250.89   0.0372   Singlet-A
H-8->LUMO (55%), H-2->L+1 (18%), HOMO->L+1 (11%) H-9->LUMO (-3%),
H-7->LUMO (-2%), H-5->L+1 (-2%), H-3->L+1 (-4%)

15   5.0874   243.71   0.0183   Singlet-A
H-9->LUMO (78%) H-4->L+1 (9%), HOMO->L+1 (4%)

16   5.1281   241.77   0.0173   Singlet-A
H-4->L+1 (69%)   H-9->LUMO (-6%), H-6->L+1 (8%), H-2->L+2 (2%)

17   5.2472   236.29   0.0287   Singlet-A
H-6->L+1 (68%)   H-9->LUMO (4%), H-4->L+1 (-6%), H-4->L+2 (-6%), H-2->L+2 (2%)

18   5.5103   225.0   0.0007   Singlet-A
H-1->L+2 (95%)   H-2->L+2 (-2%)

19   5.7358   216.16   0.1376   Singlet-A
H-2->L+2 (40%), HOMO->L+2 (12%), HOMO->L+3 (-16%)   H-6->L+1 (-4%),
H-6->L+3 (3%), H-4->L+2 (-5%), H-4->L+3 (3%), H-2->L+3 (8%)

20   5.7388   216.04   0.0015   Singlet-A
H-12->LUMO (80%) H-11->LUMO (8%), H-5->L+2 (-3%), H-1->L+3 (-3%)

21   5.7874   214.23   0.0014   Singlet-A
H-7->L+1 (82%) H-12->LUMO (3%), H-8->L+1 (4%), H-7->L+3 (-2%), H-1->L+3 (5%)

22   5.8491   211.97   0.1851   Singlet-A
H-5->L+2 (10%), H-4->L+2 (23%), H-3->L+2 (13%), HOMO->L+2 (16%) H-9->L+1 (-2%), H-8-
>L+1 (-5%), H-6->L+1 (4%), H-6->L+2 (-2%), H-6->L+3 (3%), H-1->L+3 (-9%), HOMO->L+3
(3%)

23   5.8591   211.61   0.046   Singlet-A
H-5->L+2 (45%), H-1->L+3 (-26%) H-10->LUMO (5%), H-4->L+2 (-5%), H-3->L+2 (-3%),
HOMO->L+2 (-4%)

24   5.8705   211.2   0.0028   Singlet-A
H-10->LUMO (89%) H-3->L+2 (4%)

25   5.8956   210.3   0.0379   Singlet-A
H-4->L+2 (-15%), H-3->L+2 (71%) H-10->LUMO (-3%)

26   5.9172   209.53   0.0015   Singlet-A
H-5->L+2 (38%), H-1->L+3 (50%) H-12->LUMO (4%), H-7->L+1 (-4%)

27   5.9876   207.07   0.0719   Singlet-A
H-8->L+1 (80%) H-7->L+1 (-3%), HOMO->L+2 (3%), HOMO->L+3 (3%)

28   6.0182   206.02   0.102   Singlet-A
H-2->L+2 (-22%), HOMO->L+2 (35%) H-4->L+2 (-7%), H-4->L+3 (-9%), H-3->L+2 (-4%), H-2-
>L+3 (9%)

29   6.0755   204.07   0.002   Singlet-A
H-14->LUMO (58%), H-11->LUMO (31%) H-12->LUMO (-6%)

30   6.1206   202.57   0.0824   Singlet-A
H-9->L+1 (61%), HOMO->L+3 (15%) H-11->LUMO (4%), H-6->L+2 (-7%), H-4->L+3 (3%)

First 30 excited triplet states

No.   Energy (eV)   Wavelength (nm)   Osc. Strength Symmetry
Major and minor contributions (%)

1   2.6611   465.92   0.0   Triplet-A
H-1->LUMO (97%)   H-5->L+1 (6%), H-2->LUMO (-2%)

2   2.8898   429.04   0.0   Triplet-A
H-6->LUMO (-14%), H-4->LUMO (-18%), HOMO->LUMO (55%), H-6->L+2 (4%),
H-4->L+2 (2%), H-3->LUMO (-3%), H-2->LUMO (-8%), H-2->L+1 (-6%), H-2->L+3 (-4%)

3   2.9379   422.02   0.0   Triplet-A
H-6->LUMO (52%), HOMO->LUMO (28%), H-9->LUMO (7%), H-8->LUMO (3%),
H-4->LUMO (7%), H-4->L+1 (8%), H-4->L+3 (-3%), H-2->L+1 (3%), HOMO->L+1 (4%),
HOMO->L+2 (6%)

4   2.9407   421.61   0.0   Triplet-A
H-5->LUMO (93%), H-1->L+1 (10%), H-1->L+9 (-2%)

5   3.0455   407.11   0.0   Triplet-A
H-2->LUMO (82%), HOMO->LUMO (10%), H-6->LUMO (-8%), H-4->LUMO (3%)

6   3.3068   374.94   0.0   Triplet-A
H-6->LUMO (-18%), H-4->LUMO (69%), H-2->LUMO (-11%) HOMO->LUMO (2%)

7   3.8419   322.72   0.0   Triplet-A
H-3->LUMO (94%)   H-4->LUMO (-3%)

8   3.8863   319.03   0.0   Triplet-A
H-6->L+1 (-10%), H-4->L+1 (57%), HOMO->L+1 (12%) H-6->LUMO (-7%), H-6->L+3 (2%),
H-4->L+3 (-9%), H-2->L+3 (-2%), HOMO->LUMO (-5%), HOMO->L+3 (-3%)

9   3.9207   316.23   0.0   Triplet-A
H-2->L+1 (61%), H-2->L+3 (21%) H-6->LUMO (-8%), H-4->LUMO (-3%), H-4->L+3 (-3%),
H-2->L+2 (-3%), HOMO->L+1 (8%)

10   4.2931   288.8   0.0   Triplet-A
H-4->L+1 (-12%), H-2->L+1 (-12%), HOMO->L+1 (69%), H-6->L+3 (-5%), H-3->L+1 (-2%)

11   4.4789   276.82   0.0   Triplet-A
H-5->LUMO (-10%), H-1->L+1 (85%), H-2->L+1 (-2%)

12   4.5572   272.06   0.0   Triplet-A
H-6->L+1 (77%), H-4->L+1 (10%) HOMO->L+3 (-7%)

13   4.6471   266.8   0.0   Triplet-A
H-8->LUMO (16%), H-7->LUMO (60%), H-5->L+1 (10%), H-9->LUMO (2%),
HOMO->L+2 (-3%)

14   4.6606   266.03   0.0   Triplet-A
H-13->LUMO (13%), H-9->LUMO (26%), H-7->LUMO (-17%), HOMO->L+2 (-19%)
H-8->LUMO (9%), H-6->L+8 (3%), H-4->L+2 (2%), H-2->L+2 (4%)

15   4.8168   257.4   0.0   Triplet-A
H-7->LUMO (-17%), H-5->L+1 (72%), H-1->LUMO (-3%)

16   4.8388   256.23   0.0   Triplet-A
H-8->LUMO (33%), HOMO->L+2 (27%), H-13->LUMO (-3%), H-9->LUMO (9%),
H-6->LUMO (-4%), H-5->L+1 (-6%), H-4->L+2 (-2%), H-2->L+1 (-2%), H-2->L+2 (-4%)

17   4.8887   253.61 0.0   Triplet-A
H-3->L+1 (92%)   H-4->L+1 (-3%)

18   4.9681   249.56   0.0   Triplet-A
H-9->LUMO (52%), H-8->LUMO (-36%) H-7->LUMO (3%), HOMO->L+2 (3%)

19   5.1746   239.6   0.0   Triplet-A
H-18->LUMO (10%), H-4->L+2 (-19%), H-2->L+2 (41%), H-13->L+1 (4%), H-6->L+2 (6%),
H-6->L+9 (-2%), H-4->L+3 (-4%), H-2->L+8 (6%), HOMO->L+3 (7%)

20   5.2801   234.81   0.0   Triplet-A
H-4->L+2 (36%), H-2->L+2 (25%), HOMO->L+2 (21%) H-18->LUMO (-3%), H-2->L+1 (3%)

21   5.3637   231.15   0.0   Triplet-A
H-6->L+2 (58%), H-13->LUMO (-2%), H-6->L+3 (3%), H-4->L+1 (-3%), H-4->L+2 (2%), H-4-
>L+8 (2%), H-2->L+1 (3%), H-2->L+2 (-6%), H-2->L+3 (-7%), HOMO->L+2 (-2%), HOMO-
>L+8 (-4%)

22   5.3842   230.28   0.0   Triplet-A
H-1->L+2 (93%), H-2->L+2 (-3%)

23   5.545   223.6   0.0   Triplet-A
H-4->L+2 (19%), H-4->L+3 (-10%), H-2->L+3 (24%), HOMO->L+3 (20%), H-6->L+2 (3%), H-2-
>L+1 (-9%), HOMO->L+1 (-2%)

24   5.5701   222.59   0.0   Triplet-A
H-12->LUMO (76%), H-5->L+2 (-11%), H-11->LUMO (7%)

25   5.5996   221.41   0.0   Triplet-A
H-13->LUMO (57%), HOMO->L+2 (10%) H-22->LUMO (2%), H-18->L+1 (2%), H-9->LUMO (-
3%), H-6->L+2 (9%), H-4->L+2 (-3%), H-2->L+3 (4%)

26   5.6487   219.49   0.0   Triplet-A
H-7->L+1 (72%), H-1->L+3 (10%) H-8->L+1 (8%), H-7->L+3 (-3%)

x

27   5.663   218.94   0.0   Triplet-A
H-2->L+3 (33%), HOMO->L+3 (-24%)   H-18->LUMO (-5%), H-13->LUMO (-6%), H-7->L+1
(-2%), H-6->L+2 (2%), H-4->L+2 (-4%), H-2->L+1 (-2%), H-2->L+2 (7%), HOMO->L+2 (-3%)

28   5.7387   216.05   0.0   Triplet-A
H-5->L+2 (-41%), H-1->L+3 (42%) H-12->LUMO (-6%), H-7->L+1 (-6%)

29   5.7787   214.55   0.0   Triplet-A
H-9->L+1 (20%), H-8->L+1 (23%), HOMO->L+3 (-11%) H-18->LUMO (6%), H-10->LUMO (-
4%), H-6->L+2 (-5%), H-4->L+1 (-7%), H-4->L+2 (3%), H-4->L+3 (-6%)

30   5.8417   212.24   0.0   Triplet-A
H-3->L+2 (90%), H-4->L+2 (-4%)

Note that all the transitions $S_0 \rightarrow T_1$ show a null oscillator strength, because they are forbidden by the symmetry rules.
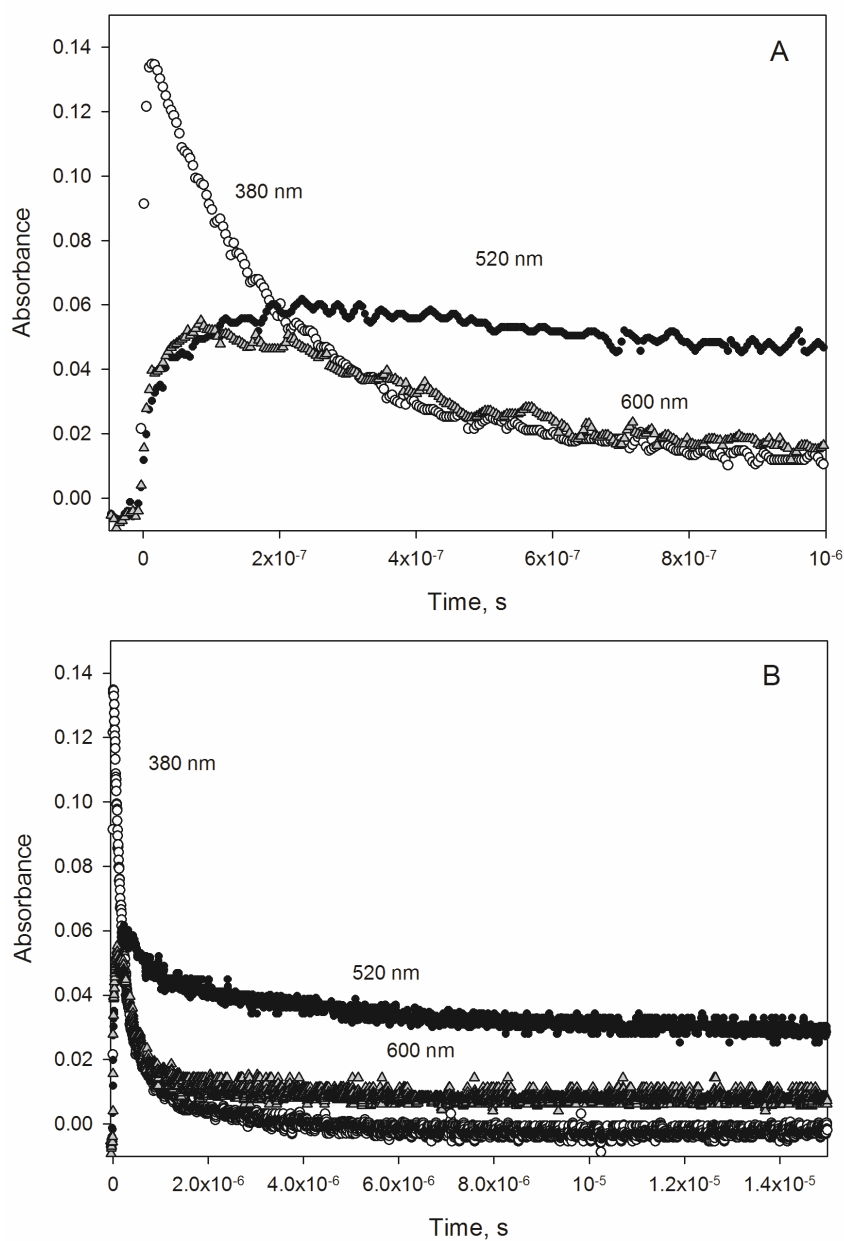
Figure ESI-3. Absorbance traces of transient species formed after the laser pulse (355 nm, 45 mJ), in the presence of 0.1 mM AQ2S at pH 6.5. Monitored transient species were: AQ2S triplet state (380 nm), B (520 nm) and C (600 nm). Time scale after laser pulse: 1 µs (**A**) and 15 µs (**B**).
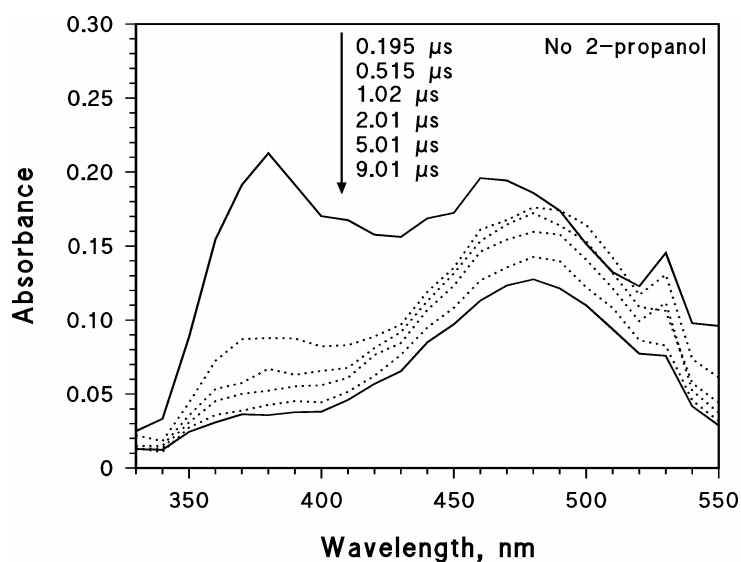
Figure ESI-4. Time trend of the absorption spectra of the transient species formed by laser pulse irradiation (355 nm, 45 mJ) of 0.1 mM AQ2S. The experiments were carried out in aerated solution, at 295 ± 2 K and pH 6.5.
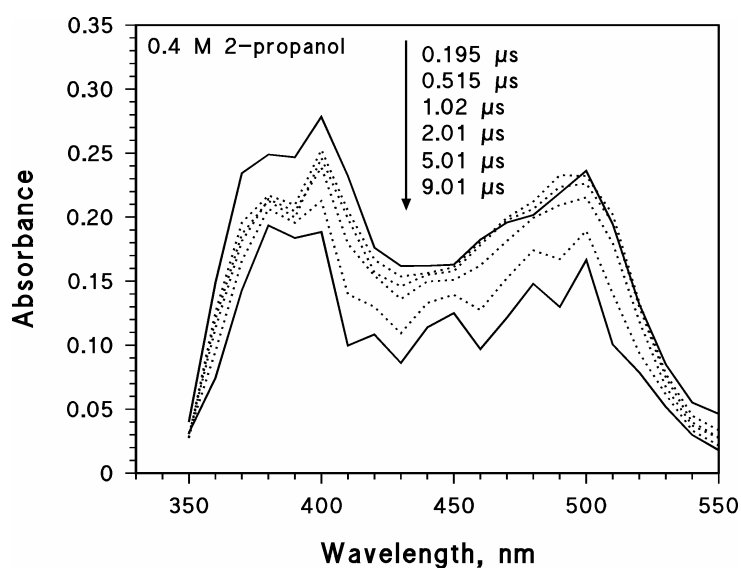
Figure ESI-5. Time trend of the absorption spectra of the transient species formed by laser pulse irradiation (355 nm, 45 mJ) of 0.1 mM AQ2S and 0.4 M 2-propanol. The experiments were carried out in aerated solution, at 295 ± 2 K and pH 6.5.
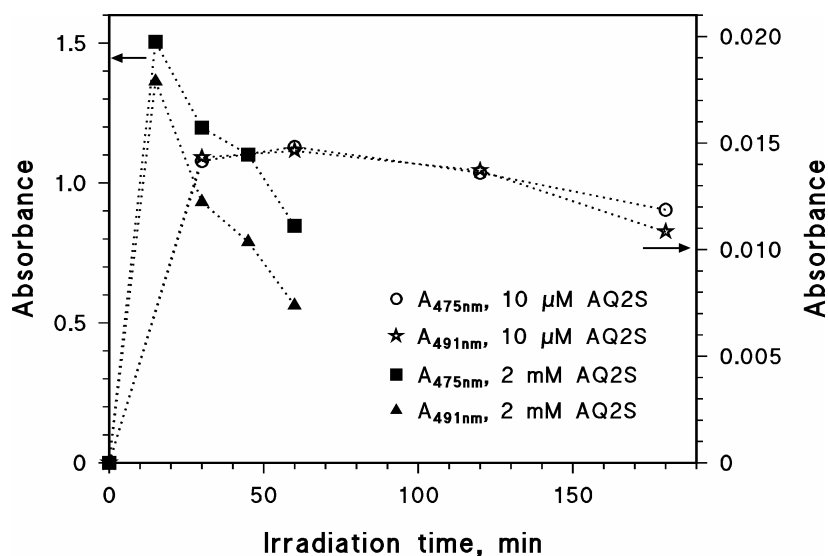
Figure ESI-6. Time trend of the absorbance (measured over an optical path length $b = 1$ cm) upon irradiation of AQ2S solutions, adjusted to pH 12 with NaOH after irradiation. Left Y-axis: absorbance with 2 mM initial AQ2S. Right Y-axis: absorbance with 0.10 µM initial AQ2S. The experiments were carried out in aerated solution at 295 ± 2 K. UVA irradiation took place under the Philips TLK 05 lamp.